Experimental Eye Research 125 (2014) 183–192

Contents lists available at ScienceDirect

Experimental Eye Research

journal homepage: www.elsevier.com/locate/yexer

IL-6 as a corneal wound healing mediator in an *in vitro* scratch assay

Isabel Arranz-Valsero [a, b], Laura Soriano-Romaní [a, b], Laura García-Posadas [a, b], Antonio López-García [a, b], Yolanda Diebold [a, b, *]

[a] Ocular Surface Group-IOBA, University of Valladolid, Valladolid, Spain
[b] Biomedical Research Networking Center on Bioengineering, Biomaterials and Nanomedicine (CIBER-BBN), Spain

ARTICLE INFO

Article history:
Received 20 March 2014
Accepted in revised form 15 June 2014
Available online 24 June 2014

Keywords:
corneal cells
wound healing
cytokine stimulation
IL-6
IL-10

ABSTRACT

Corneal healing process under inflammatory conditions is not fully understood. We aimed at determining the effect of an inflammatory (presence of IL-6) or anti-inflammatory (presence of IL-10) environment and a mixture of both in the expression of IL-6 signaling pathway mediators, and on corneal wound healing in an *in vitro* scratch assay. For that purpose, human corneal epithelial cells were cultured until confluence. The effect of IL-6 (10 ng/ml), IL-10 (20 ng/ml) or IL-6 + IL-10 exposure on the expression of IL-6R, gp130, and STAT3 was determined by Western blotting and quantitative PCR, at different time points. The monolayer was mechanically wounded using a sterile 10 μl pipette tip. Wound healing rate in the presence or absence of these cytokines was measured immediately after cytokine exposure and after 4, 8, and 24 h. The effect of mitomycin C on wound healing rate, in control and IL-6-stimulated cells, was also evaluated. Detection of proliferative cells was performed with an EdU imaging kit. For the visualization of migrating cells, cold methanol-fixed cells were incubated with an α-actinin antibody. For the statistical analysis a two-factor design of experiment method was applied. Levene test was used to contrast equality of variances. If variances were equal, ANOVA was performed to test the equality of means. If variances were not equal, a Mood's median test was performed. We observed that IL-6 and IL-10 stimulation, and their combination, increased gp130 production at different time points. STAT3 production was increased in IL-6-stimulated cells, at 72 h. An increase in pSTAT3 production was found in IL-6- and IL-10-stimulated cells, that was sustained in time in IL-6 + IL-10 co-stimulated cultures. Scraped areas had an initial width of 570.57 ± 75.82 μm. In IL-6-exposed cells wound healing closure was faster than in control cells or IL-10-exposed cells. After 8 h, wound width in IL-10-exposed cells, was also significantly smaller than that of control cells. Cells exposed to IL-6 + IL-10 had the slowest wound healing rate, similar to control cells. Wounds were closed after 24 h regardless the experimental condition. Mitomycin C exposure increased the wound closure rate in every experimental condition. No significant differences in the percentage of proliferative cells at the edge of the scratch and in distant areas of the monolayer were found. At the edge of the scratch, some actin filaments of non-proliferative cells were directed through the cell-free area, independently of the stimulating condition. In conclusion, the presence of IL-10 and, most importantly, of IL-6, increased the wound healing rate in an *in vitro* corneal wound healing model. The combination of both cytokines did not have a synergistic action in wound healing. In our model, wound closure was the result of the combination of cell proliferation and cell migration.

1. Introduction

The ability of the cornea to heal and maintain its clarity has paramount importance in preserving the eyesight. Corneal opacity results from the formation of a scar in corneal tissues after different insults, such as trauma, eye surgery, or inflammatory diseases of the anterior part of the eye (Aurora, 1979; Seibold et al., 2012; Yang et al., 2013). In the ocular surface, a pathologic wound healing process, along with local inflammation and neovascularization can induce failure in the functional recovery of the ocular surface tissues, which can lead to corneal blindness.

The inflammatory response triggered during wound healing involves several cytokines secreted by epithelial cells or immune

* Corresponding author. IOBA-University of Valladolid, Edificio IOBA, Campus Miguel Delibes, Paseo de Belén 17, 47011 Valladolid, Spain. Tel.: +34 983 18 47 50; fax: +34 983 18 47 62.
E-mail address: yol@ioba.med.uva.es (Y. Diebold).

http://dx.doi.org/10.1016/j.exer.2014.06.012
0014-4835/

cells. The inflammatory response is usually meant to be in benefit of regeneration (Benowitz and Popovich, 2011; Filbin, 2006; Lu and Richardson, 1991). Specifically for the eye, the pro-inflammatory cytokine interleukin (IL)-6 stimulates cell migration of rabbit corneal epithelial cells and wound closure in an *in vitro* wound healing model (Nakamura and Nishida, 1999). IL-6 is a multifunctional cytokine related to a wide range of inflammatory conditions in the ocular surface, such as dry eye syndrome. It has been related to pain, tear film production and stability, and the integrity of the ocular epithelium (Enriquez-de-Salamanca et al., 2010), and its levels are found elevated in tears from dry eye patients. Following IL-6 dimerization, the signal transduction engages two specific transmembrane receptors (IL-6R) and two transmembrane glycoprotein (gp)130, leading to their dimerization and hexameric complex formation (Ward et al., 1996). Then, the activated Janus kinases (JAK) self-phosphorylate and induce the phosphorylation of the receptor complex, and the signal transducer and activator of transcription-3 (STAT3) (Darnell, 1997; Subramaniam et al., 2013). The activated STAT3 dimer enters the nucleus and operates as a transcription regulator. STAT3 has been evaluated as a possible therapeutic target in cancer and skeletal muscle wasting (Bonetto et al., 2012).

On the other hand, IL-10 is a cytokine with an immunosuppressive role in human cells (de Waal Malefyt et al., 1991), and develops an immunomodulatory role in ocular inflammatory diseases (Ghasemi et al., 2012). Increased IL-10 levels have been found in patients with glaucoma (Baudouin et al., 2004), primary intraocular lymphoma (Cassoux et al., 2007), and corneal graft rejection(van Gelderen et al., 2000). Besides, topical treatment with IL-10 improved the recovery of stromal herpetic keratitis patients (Boorstein et al., 1994). In addition, our group reported that IL-10 stimulation has corneal epithelial barrier protective effects in vitro (Contreras-Ruiz et al., 2012). With these data in mind, we considered that IL-10 is likely to improve corneal re-epithelization after an injury, as happens in wound healing.

Recent studies of wound healing in human fetal tissue revealed that a fast healing process is scarless, thanks to the recruitment of fibroblasts (Coolen et al., 2010). A slower healing process leads to the deposition of extracellular matrix elements and the transition of fibroblasts to myofibroblasts, producing pathology and even fibrosis (Eckes et al., 2000; Micera et al., 2006). In the ocular surface, this may suppose the difference between corneal blindness and normal vision. Besides, an elevated proliferation rate in wounded tissues may lead to scarring and, therefore, to the loss of vision. To minimize this process, mitomycin C (MMC), a proliferation inhibitor, is frequently administered after ocular surgical procedures to avoid scarification of the remaining wound (Lockwood et al., 2013). Moreover, recent studies have proved that an anti-inflammatory treatment effectively reduced corneal opacification during corneal injury (Ferrari et al., 2013; Oh et al., 2010).

Nevertheless, the exact contribution of several cytokines, such as IL-6 and IL-10, and their signaling pathways mediators, in corneal wound healing is not fully understood. The purpose of this study was to evaluate the effect of the treatment with IL-6 and IL-10 on IL-6 signaling pathway mediators and on corneal re-epithelization, in an *in vitro* model of wound healing.

2. Materials and methods

2.1. Materials

Tissue culture plastics, including multichamber Permanox™ slides were obtained from Nunc (Roskilde, Denmark). Culture medium and supplements, Alexa fluor 488 donkey-anti-mouse secondary antibody (Ab) for immunofluorescence analysis, SuperScript VILO cDNA Synthesis Kit, and the Click-iT EdU Alexa-Fluor647 imaging kit were purchased from Invitrogen-Gibco (Inchinnan, UK). Human recombinant IL-6 and IL-10 were from PeproTech (London, UK). Enzyme-linked immunosorbent assay (ELISA) kits for soluble (s)gp130 and sIL-6 receptor (R) were from Diaclone (Besançon, France). Mitomycin C (MMC), donkey serum, Laemmli sample buffer, protease inhibitors, Hoechst33342, and Tween-20 were from Sigma–Aldrich (St. Louis, MO). The bicinchoninic acid (BCA) protein quantification method was from Pierce (Rockford, IL). Materials used for sodium dodecyl sulfate–polyacrylamide gel electrophoresis (SDS–PAGE) and Western blotting (WB), including analysis software, were purchased from Bio-Rad (Hercules, CA). Low fat milk powder, α-actinin primary Ab, and goat anti-rabbit secondary Ab were obtained from Santa Cruz Biotechnology (Santa Cruz, CA). IL-6R primary Ab was from Abcam (Cambridge, UK), gp130 primary Ab was from R&D Systems (Minneapolis, MN), and STAT3 and pSTAT3 primary Abs were from Cell Signaling (Beverly, MA). Donkey anti-mouse affine pure peroxidase-conjugated immunoglobulin came from Jackson ImmunoResearch Laboratories (West Grove, PA). Vectashield medium was from Vector Laboratories (Burlingame, CA). Phase contrast or fluorescence images were obtained with an epifluorescence microscope DMI 6000B from Leica Microsystems (Wetzlar, Germany). Image analysis was performed using the Leica LAS AF 3000 imaging software. All the materials for mRNA extraction, purification, and quantification, as well as 2X SYBR Green Real-time PCR Master Mix were from Qiagen (Hilden, Germany). IL-6R, gp130, and STAT3 validated primer pair oligonucleotides were from Origene Technologies (Rockville, MD). Real-time, reverse-transcription quantitative polymerase chain reaction (qPCR) was performed in an Applied Biosystems 7500 Real-Time PCR System (Foster City, CA).

2.2. Human corneal epithelial cell line

A human corneal epithelial (HCE) cell line (Araki-Sasaki et al., 1995) was cultured in Dulbecco's Modified Essential Medium DMEM/F-12 + GlutaMAXTM-I supplemented with 10% fetal bovine serum (FBS), 100 U/ml penicillin, and 0.1 mg/ml streptomycin. Cells were maintained at 37 °C in a 5% CO_2 atmosphere, and the culture medium was changed every other day. Daily observations were done by phase contrast microscopy.

2.3. Cytokine stimulation

HCE cells were grown to confluence on 12-well Permanox™ plates. They were then maintained for 24 h in DMEM without supplements, prior the exposure to the following cytokines: IL-6 (10 ng/ml) or IL-10 (20 ng/ml) in DMEM without supplements, or a combination of both in the same concentrations. Doses of the stimulatory cytokines used were chosen based on previous publication by our group and others (Contreras-Ruiz et al., 2012; Enriquez-de-Salamanca et al., 2008). Cell culture supernatants were collected at different time points and the secretion of sIL-6R and sgp130 was measured by ELISA, according to the manufacturer's instructions. Cell lysates obtained at the same time points were used for IL-6R, gp130, STAT3, and pSTAT3 protein production analysis by SDS-PAGE and WB, or mRNA expression measurement with qPCR.

2.4. In vitro scratch assay

HCE cells were grown to confluence on 24-well Permanox™ plates. Consistently shaped wounds were made using a sterile

Table 1
Antibodies and detection conditions for the immunoblotting assay.

Protein	Blocking solution	Primary Ab	Reference	Dilution	Incubation time	Incubation temp. (°C)	Secondary Ab	Reference	Dilution	Incubation time	Incubation temp. (°C)
IL-6R											
	4% donkey serum and 5% BSA in TBS-T	Rabbit anti-IL-6R	ab128008	1:200	ON	4	Goat anti rabbit	sc-2004	1:2000	1 h	RT
GP130											
	2% BSA in TBS-T	Mouse anti-GP130	MAB2281	1:160	ON	4	Donkey anti mouse	715-035-150	1:5000	1 h	RT
STAT3											
	4% goat serum and 5% BSA in TBS-T	Rabbit anti-STAT3	9132S	1:2000	ON	4	Goat anti rabbit	sc-2004	1:2000	1 h	RT
pSTAT3											
	4% goat serum and 5% BSA in TBS-T	Rabbit anti-pSTAT3	9145P	1:1000	ON	4	Goat anti rabbit	sc-2004	1:2000	1 h	RT
GAPDH											
	4% goat serum and 5% BSA in TBS-T	Mouse anti-GAPDH	sc-51905	1:1000	ON	4	Donkey anti mouse	715-035-150	1:5000	1 h	RT
α-actinin											
	4% donkey serum and 5% non-fat milk in TBS-T	Mouse anti-α-actinin	sc-17829	1:500	ON	4	Donkey anti mouse	715-035-150	1:5000	1 h	RT

Ab, antibody; BSA, bovine serum albumin; TBS-T, tris buffered saline + 0.05% Tween20; ON, over night; RT, room temperature.

10 μl pipette tip across each well, creating a cell-free area, based on the technique described by Liang et al. (Liang et al., 2007). Cultures were gently washed with DMEM/F12 to remove loose cells. The cells were then exposed to the following cytokines: IL-6 (10 ng/ml), IL-10 (20 ng/ml), or a mix of both in the same concentrations, in culture medium supplemented with 1% FBS. Cells for control conditions were also scratched, washed, and maintained in culture medium supplemented with 1% FBS after the scratch.

Immediately after the scratch and at 4, 8, and 24 h, at least four images of the scraped area were captured using phase contrast microscopy. The remaining wounded area and the scratch width at six different points per image were measured. Three independent experiments were performed, using three wells for each stimulating condition. The same scratched area was selected for the measurements at each time of study.

2.5. Protein detection by electrophoresis and Western blotting

Cells exposed to different cytokines were washed with phosphate buffered saline (PBS) and homogenized in ice-cold radioimmunoprecipitation assay (RIPA) buffer: (10 mM Tris–HCl [pH 7.4], 150 mM NaCl, 1% deoxycholic acid, 1% Triton X-100, 0.1% SDS, and 1 mM EDTA) supplemented with protease inhibitors (100 μL/mL phenylmethylsulfonyl fluoride, 6 μL/mL aprotinin, and 100 nM sodium orthovanadate). The samples were then incubated for 30 min on ice and centrifuged at 15,000 g for 30 min at 4 °C. Supernatants were collected and total cell protein was measured by the BCA method, which was compatible with the buffer used for homogenization. Bovine serum albumin (BSA) was used as the standard.

Protein in cell lysates were mixed 1:1 with Laemmli Simple Buffer and boiled for 5 min. Equal amounts of proteins (10 μg/lane) were separated on 8% acrylamide gels with SDS-PAGE (15 min at 70 V and 1.5 h at 110 V), with a 4% stacking gel. The proteins were then electrophoretically transferred to nitrocellulose membranes (1.5 h at 350 mA). The membranes were incubated in blocking solution for 1 h at room temperature (RT), followed by the incubation with the primary Abs diluted in tris buffered saline + 0.05% Tween 20 (TBS-T), overnight at 4 °C. The membranes were washed three times with TBS-T, and incubated with the corresponding secondary Abs diluted in TBS-T. Blocking conditions for each protein detection, along with primary and secondary Abs are included in Table 1. Visualization of the specific protein bands was accomplished using an enhanced chemiluminescence detection system from Bio-Rad. Blots were incubated with the detection reagent for 5 min and then visualized by the chemiluminescence method (ChemiDoc XRS). Images were analyzed using the Quantity One software (Bio-Rad).

2.6. Quantification of mRNA expression levels by qPCR

Cell lysates were prepared from HCE cells and RNA was isolated and purified using the small chromatography columns from the *RNAeasy-columns* extraction kit, following the manufacturer's instructions. Samples were incubated with DNase for 10 min at RT, to avoid the further amplification of genomic DNA. Total RNA was quantified using the Quant-it™ *RNA Assay Kit*, with the Qubit fluorometer. A total of 1 μg of purified RNA was used for each reaction of reverse transcription with the Super Script® VILO™ cDNA synthesis Kit, with the following amplification parameters: 10 min at 25 °C, 2 h at 42 °C, and 5 min at 85 °C.

IL-6R, gp130, and STAT3 mRNA levels were quantified with qPCR, using validated primer pair oligonucleotides. Primer oligonucleotides were synthesized for the house-keeping ribosomal 18S rRNA (sense: 5'-ACTCAACAGGGGAAACCTCAGC-3'; antisense: 5'-CGCTCCACCAACTAAGAACGG-3'). The PCR reaction was carried out in a volume of 20 μl using 10 μl of 2 × SYBR Green Realtime PCR Master Mix, 0.4 μg of synthesized cDNA, and the specific primer pair at 5 nM. The amplification procedure consisted in 2 min incubation at 50 °C, 10 min incubation at 95 °C and 40 cycles of denaturation at 95 °C for 15 s, and annealing and elongation at 60 °C for 1 min, for the validated primers. For the detection of 18S rRNA, the amplification procedure consisted in 2 min incubation at 50 °C, 3 min incubation at 94 °C and 40 cycles of denaturation at 94 °C for 20 s, annealing at 59 °C for 33 s and elongation at 72 °C for 40 s. The fluorescence signal was digitally collected after each cycle of 72 °C. The semi-quantitative ΔΔCt method was used to analyze the relative gene expression of each sample, using the 18S rRNA signal for normalization. Controls included no-template controls and no-reverse-transcription controls. After each PCR, samples were subjected to a temperature ramp with continuous fluorescence monitoring for melting curve analysis to verify that the fluorescence signal was due to the amplification of a single fragment.

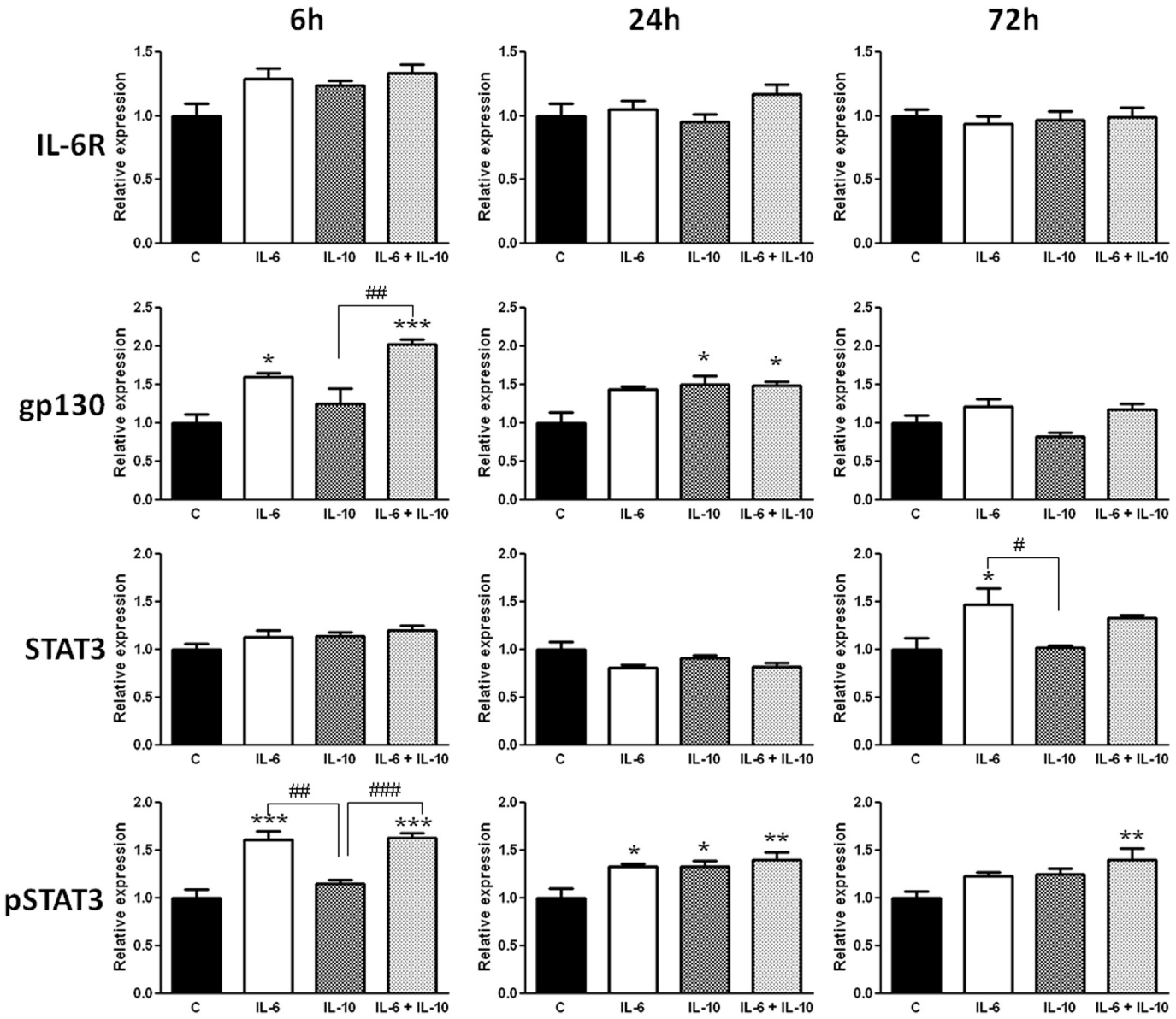

Fig. 1. Interleukin 6 receptor (IL-6R), glycoprotein 130 (gp130), and signal transduction and activator of transcription-3 (STAT3) unactivated, or phosphorylated (pSTAT3) production by HCE cells exposed to IL-6 and/or IL-10, at 6, 24 or 72 h, determined by SDS-PAGE and Western blotting. Bars represent the mean value of duplicates from three independent experiments. Values are expressed as mean ± SEM, and statistical significance, when compared to control unstimulated cells, is indicated with asterisks ($^{*}p \leq 0.05$; $^{**}p \leq 0.01$; $^{***}p \leq 0.001$). Significant differences between different groups are indicated by #($p \leq 0.05$), ##($p \leq 0.01$), or ###($p \leq 0.001$).

2.7. Proliferation inhibition with mitomycin C

HCE cells were grown to confluence on 24-well Permanox™ plates. Cells were then treated with 10 μg/ml of MMC in culture medium supplemented with 1% FBS, for 2 h. Afterwards, cells were washed with PBS and incubated in culture medium supplemented with 1% FBS for 16 h. One linear scratch was made and the same procedure explained above for the scratch assay was performed in MMC-pretreated cells.

2.8. Proliferation detection with EdU

HCE cells were grown until confluence on 8-well Permanox™ multichamber slides. One linear scratch was made and the same procedure explained above for the scratch assay was performed. Cells were incubated with a solution containing 10 μM of the thymine analog EdU alone or along with the stimulating conditions (IL-6, IL-10, or a combination of both). For EdU detection, samples were processed following the manufacturer's instructions. Briefly, cells were fixed in 3.7% formaldehyde in PBS for 15 min at RT. Permeabilization was performed with a 0.5% Triton X-100 solution in PBS, for 20 min at RT. Then, the samples were incubated with the reaction mix for 30 min. Nuclei were stained with a 1:1500 Hoechst 33342 solution in PBS, for 15 min at RT.

Slides were mounted in Vectashield medium, and the preparations were viewed in a Leica fluorescence microscope. Three independent experiments were performed. For each stimulating condition, five different fields were imaged in the edge of the scratch and eight fields were imaged in distant areas of the monolayer. Total numbers of cells with blue stained-nuclei were counted in each field. Proliferative cells with EdU incorporated were identified by their red-stained nuclei, and counted. More

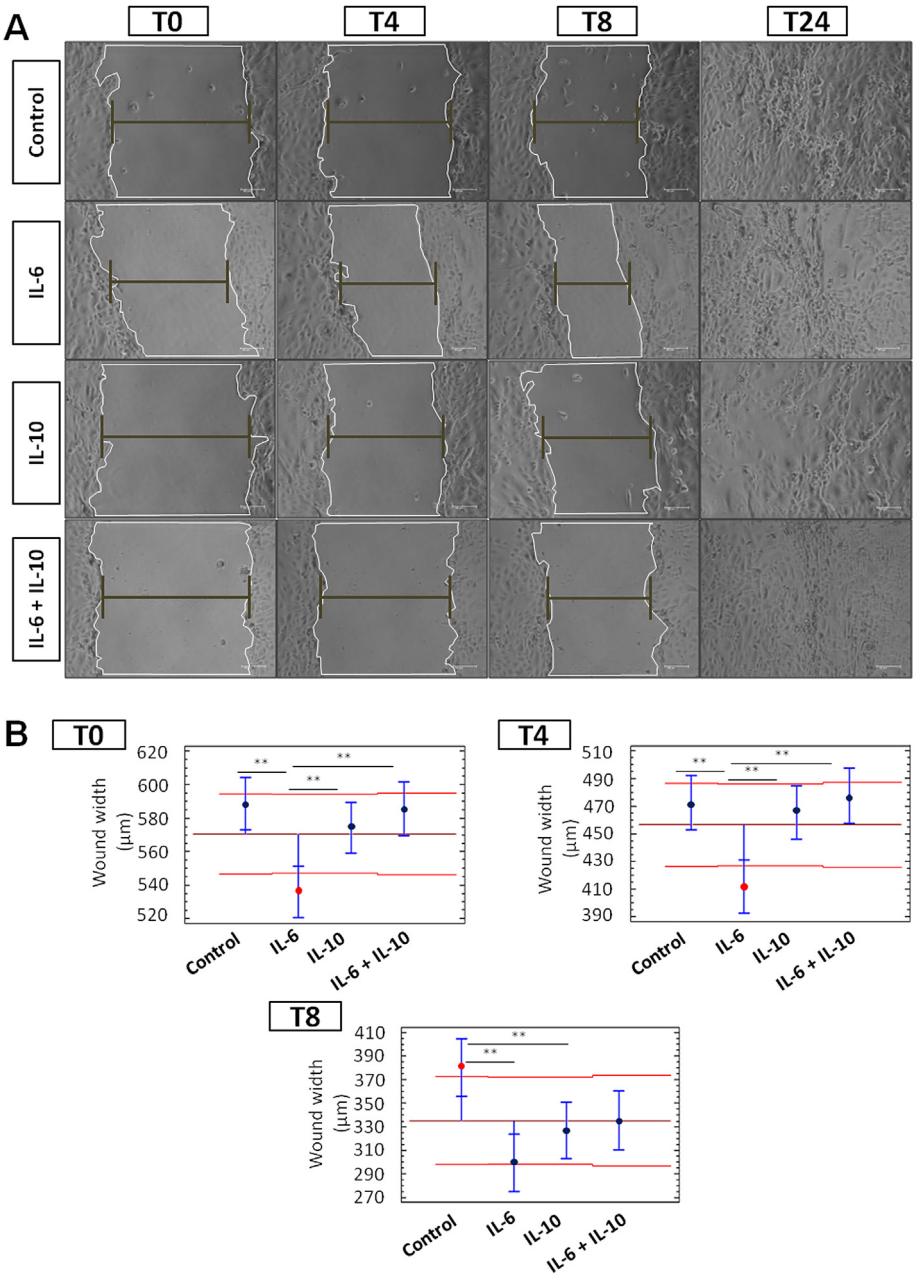

Fig. 2. Wound closure rate evaluation in the *in vitro* scratch assay. **A**. Representative micrographs of the scratch in different stimulating conditions, at different times. Bar = 100 µm. **B**. Wound width at different time points in cultures exposed to different conditions. Means located above or under the red bars are significantly different from the total mean (brown bar) ($p \leq 0.05$). Statistically significant differences between samples are indicated by **($p \leq 0.01$). (For interpretation of the references to color in this figure legend, the reader is referred to the web version of this article.)

than 500 cells were counted for each condition. The mean proliferative cell percentage was obtained for the two considered areas: the edge of the scratch and peripheral areas of the cell monolayer.

2.9. Cytoskeleton staining with an α-actinin antibody

Cytoskeleton was visualized in HCE fixed cells treated as explained for EdU staining and detection. Slides were incubated 1 h at 37 °C with an α-actinin primary Ab diluted 1:50 in PBS, washed three times, and then incubated with the Alexa fluor 488 donkey-anti-mouse secondary Ab, 1:100 in PBS for 1 h at RT. Nuclei were stained with a 1:1000 Hoechst33342 solution in PBS for 10 min. Slides were mounted in Vectashield medium, and the preparations were viewed in the Leica epifluorescence microscope. Negative controls included the omission of primary Ab. All samples were prepared in duplicate, in three independent experiments.

2.10. Statistical analyses

The distance migrated by cells was measured and compared with that of the untreated control using a statistical analysis based on a two-factor design of experiments. For the interpretation of the results we used either ANOVA and Kruskal–Wallis test or Mood's median test, depending on Levene's test for homogeneity of variances. Data are expressed as mean ± SEM. A value of $p \leq 0.05$ was considered statistically significant.

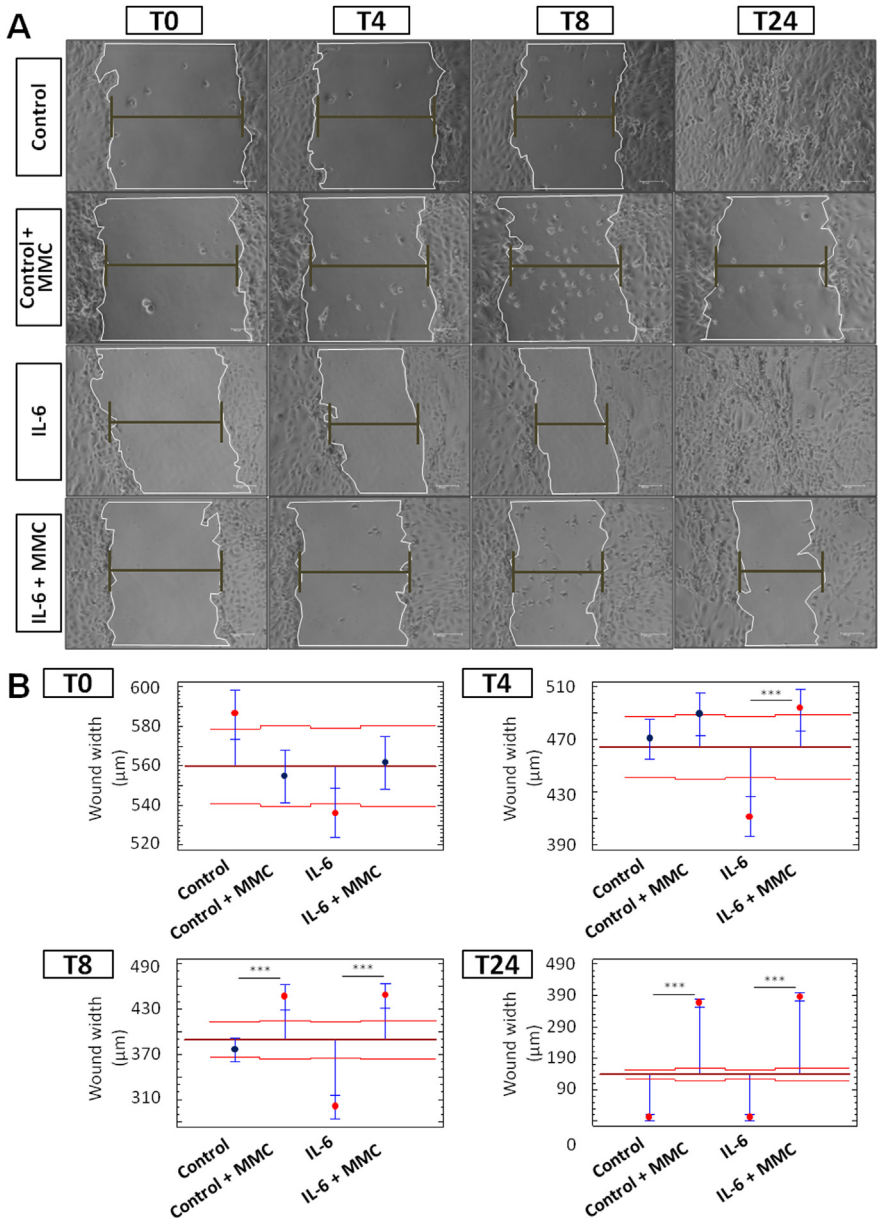

Fig. 3. Wound closure rate evaluation in the *in vitro* scratch assay, in IL-6-stimulated and control HCE cells, pre-treated or not with Mitomycin C (MMC). **A**. Representative micrographs of the scratch in the different stimulating conditions, at different times. Bar = 100 µm. **B**. Wound width at different time points in cultures exposed to different conditions. Means located above or under the red bars are significantly different from the total mean ($p \leq 0.05$). Statistically significant differences between samples are indicated by ***($p \leq 0.001$). (For interpretation of the references to color in this figure legend, the reader is referred to the web version of this article.)

3. Results

3.1. gp130, STAT3, and pSTAT3 but not IL-6R, sIL-6R or sgp130 production is modified after cytokine exposure

sIL-6R and sgp130 secretion was quantified by ELISA in supernatants of control HCE cells and of cells exposed to IL-6, IL-10, or a combination of IL-6 + IL-10. HCE cells secreted both soluble molecules in a time-dependent manner. No significant differences were found between control samples and cytokine-exposed samples (data not shown).

Aliquots of the supernatants of each condition were collected at the beginning of each scratch assay, and at 4, 8 and 24 h. Levels of sIL-6R and sgp130 were quantified by ELISA. No statistically significant differences were found for any of the stimulating conditions or at any time of study (data not shown).

IL-6R, gp130, STAT3, and pSTAT3 production was determined in cell lysates from cytokine-exposed HCE cells by SDS-PAGE and Western blotting (Fig. 1). IL-6R production in each experimental condition was similar to that of controls. gp130 production was significantly increased in IL-6- and in IL-6 + IL-10-stimulated cells, at 6 h ($p \leq 0.05$ and $p \leq 0.001$, respectively). At 24 h, gp130 production was increased in IL-10-stimulated cells ($p \leq 0.05$) and in IL-6 + IL-10-stimulated-cells ($p \leq 0.05$). At 72 h, gp130 levels remained similar to control levels in every stimulating condition. STAT3 production was increased in IL-6-stimulated cells only after 72 h ($p \leq 0.05$). On the other hand, pSTAT3 production was increased in IL-6- and IL-6 + IL-10-stimulated cells, at 6 h ($p \leq 0.001$ for both). At 24 h, pSTAT3 production was increased in IL-6-, IL-10, and IL-6 + IL-10-stimulated cells ($p \leq 0.01$, $p \leq 0.01$, $p \leq 0.001$, respectively), and at 72 h the significant increase was present only in IL-6 + IL-10-stimulated cells ($p \leq 0.01$).

The qPCR analysis of IL-6R, gp130, and STAT3 mRNA expression revealed only changes in gp130 mRNA expression, which was decreased in IL-6-stimulated cells at 24 h ($p \leq 0.05$) (data not shown).

3.2. IL-6 accelerates wound closure

Scratched areas had an initial width of 570.57 ± 75.82 μm. The rate of wound closure was different depending on cytokine exposure, but all wounds were closed after 24 h regardless of the experimental condition (Fig. 2A). Immediately after the scratch (T0) and after 4 h (T4), wounds in IL-6-exposed cells were significantly smaller than those of cells exposed to the other conditions ($p \leq 0.05$). Wound width in IL-6- or IL-10-exposed cells, but not in IL-6 + IL-10-exposed cells, was significantly smaller than that of control cells after 8 h (Fig. 2B).

3.3. Mitomycin C-treated cells have a decreased wound healing rate

Cultures pre-treated with MMC were also scratched, and the wound width was measured (Fig. 3). At T0, there were no differences in the mean wound width between MMC-treated or untreated cultures. At T4, IL-6-exposed MMC-treated cultures had a significantly higher wound width ($p \leq 0.001$) than non MMC-treated cells. At T8, MMC-treated cultures with and without IL-6 exposure had significantly higher wound width than untreated cells ($p \leq 0.001$). At T24, wounds in untreated cultures were closed, while in MMC-treated cultures wounds were still open (Fig. 3A). After 48 h, the wound was still open in MMC-treated cells. In MMC-treated cultures, large numbers of dead cells were present in the cell-free area from T8 on.

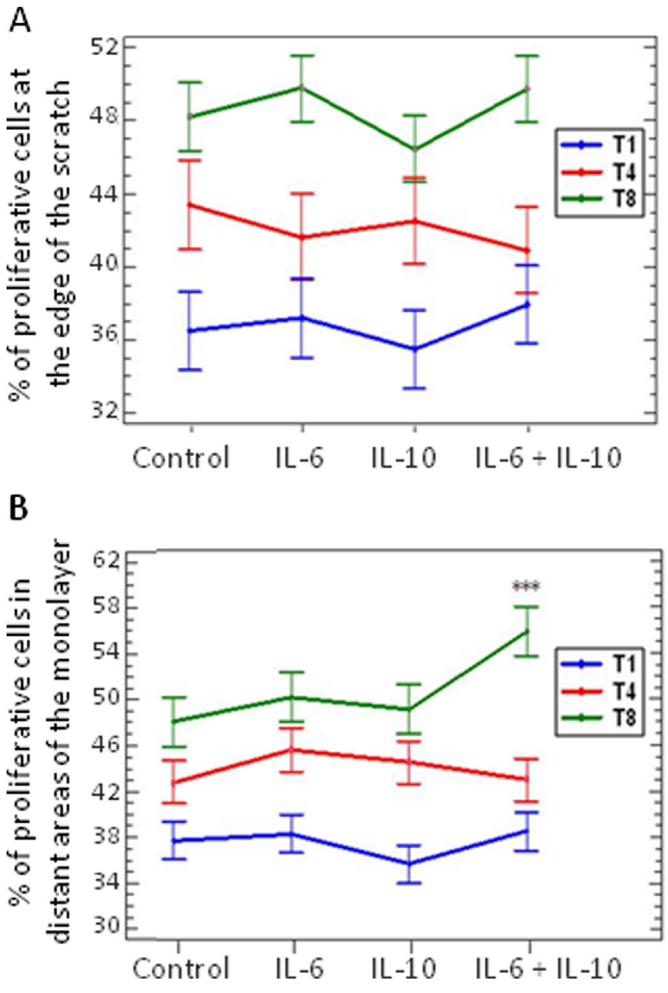

Fig. 4. Percentage of proliferative cells in the *in vitro* scratch assay, quantified through EdU detection, in **A**. the edges of the scratch or in **B**. distant areas of the monolayer, under different stimulating conditions, at different time points. Statistically significant differences respect to control conditions are indicated by ***($p \leq 0.001$).

3.4. Proliferation and migration are both involved in corneal wound healing

Scratched HCE cultures were incubated with EdU to determine the specific contribution of proliferative and non-proliferative cells to the healing process. As long as EdU was incorporated in the newly synthesized DNA, EdU detection allowed the visualization of proliferative cells. The percentage of proliferative cells in the scratch borders or in peripheral areas of the monolayer in the different stimulating conditions was measured. First, no differences were found in the percentage of proliferative cells between the edge of the scratch and the peripheral monolayer. For both, the percentage increased with time in all conditions. There was a 6% increase in proliferative cell numbers between T1 and T4, as well as between T4 and T8 ($p \leq 0.001$). A significant 7.9% increase in proliferative cell numbers was found in peripheral areas of the monolayer in IL-6 + IL-10-stimulated cells respect to control cells, at T8 ($p \leq 0.001$) (Fig. 4).

Cell migration in the scratch borders was evaluated through the visualization of cytoskeleton changes with an α-actinin antibody. At T1, some actin filaments of non-proliferative cells were directed to the cell-free area, regardless the stimulating condition. At T4, greater numbers of mostly non-proliferative cells presented actin filaments directed towards the scratched area. However at T8, this phenomenon was also observed in some proliferative cells. There were no differences in cell morphology among the different stimulating conditions (Fig. 5).

4. Discussion

Corneal injury can happen accidentally or during surgical procedures. Corneal wound healing triggers a controlled inflammatory response with the aim of preserving vision, destroying the harmful agent, and repairing damaged tissues. However, an enhanced inflammatory response can sometimes turn into a pathologic process leading to a surgery failure that, in turn, can be sight-threatening (Nathan, 2002; Ueta and Kinoshita, 2012). Currently, elevated levels of IL-6 have been related to the opacification of the posterior capsule after cataract surgery (Lewis, 2013), one of the most common surgeries in the ocular field. However, whether the presence of specific pro-inflammatory cytokines, such as IL-6, or anti-inflammatory cytokines, such as IL-10, is in benefit of a clean corneal wound closure or, on the contrary, leads to scarring and corneal haze and opacification, remains unknown.

The effect of IL-6- and IL-10-stimulation on the expression of different molecules of the IL-6 signaling pathway was firstly analyzed. Corneal epithelial cells were inflamed in a similar way as conjunctival epithelial cells were in a previous report by our group (Enriquez-de-Salamanca et al., 2008). The over-expression of pro-inflammatory factors in tears or in the ocular surface has been related to chronic inflammatory or autoimmune diseases (Leonardi et al., 2008; Mochizuki et al., 2013; Romagnani and Crescioli, 2012). As these diseases are known to degrade the quality of life of patients, the understanding of the molecular processes occurring during disease progression becomes a topic of great importance.

IL-6 is a pro-inflammatory cytokine and IL-10 often plays a role as a regulatory molecule. To determine the effect of both cytokines

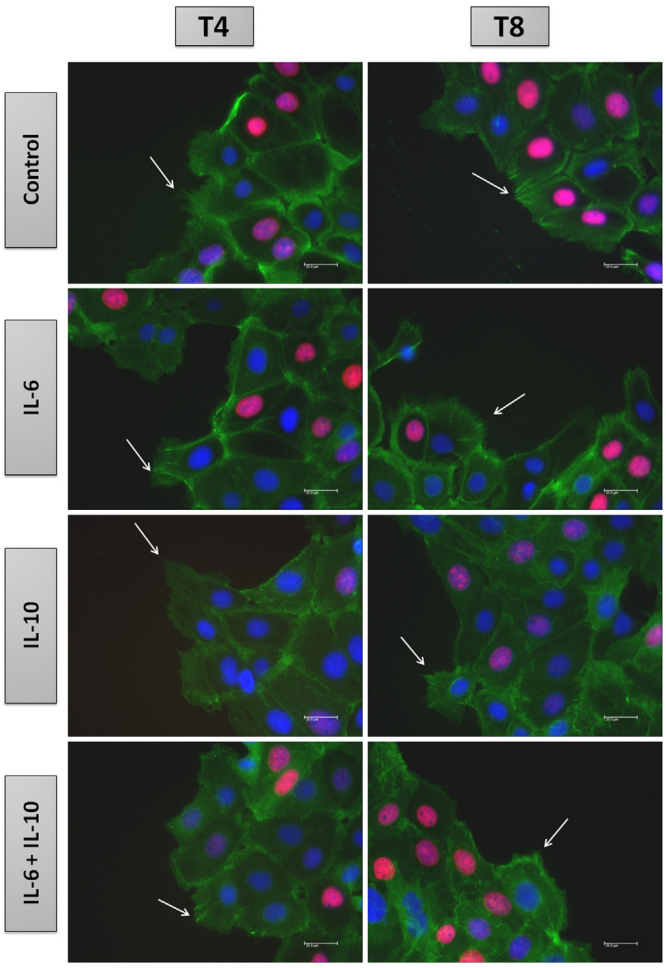

Fig. 5. Cell migration in the scratch borders under different stimulating conditions, evaluated through cytoskeleton detection with an α-actinin antibody (green). Nuclei of proliferative cells, with the EdU incorporated, were stained in red, while nuclei of non-proliferative cells were stained in blue, with Hoechst. Bar = 25 μm. (For interpretation of the references to color in this figure legend, the reader is referred to the web version of this article.)

in the IL-6 signaling pathway, the expression of membrane-bound and soluble IL-6R, membrane-bound and soluble gp130, STAT3 and activated pSTAT3 was measured. Levels of secreted protein were not statistically different respect to control in any condition. Besides, IL-6R protein or mRNA levels were unchanged in stimulated or control cells. On the other hand, gp130 production was enhanced by IL-6, and IL-10 stimulation. The combination of IL-6 + IL-10 stimulation also led to an increase in gp130 production. The role of IL-10 as a positive regulator of gp130 via STAT3 has been described in mast cells of mice (Traum et al., 2012). IL-10 signaling involves STAT3 activation, as does IL-6 signaling. Although IL-10 signaling is independent of gp130, the increase of pSTAT3 after IL-10 stimulation would lead to a positive regulation of gp130 production.

Gp130 mRNA but not protein expression was decreased at 24 h. Although these data may seem contradictory, one has to take in mind that the results of protein and mRNA expression give information about different points of the transcription/translation pathway. Thus, the apparent discrepancies could be explained. For gp130 expression, protein level was increased in every stimulating condition by maintaining constant mRNA levels, except after IL-6 stimulation, which was the only condition that produced a decrease in mRNA levels.

On the other hand, gp130 expression is regulated by SOCS3 protein, which inhibits cytokine signaling via gp130 and the JAK/STAT pathway (Silver and Hunter, 2010). The soluble fraction of gp130 (sgp130) is a well-known antagonist of IL-6 (Heinrich et al., 1998). In our results, any significant changes were found in sgp130 secretion in IL-6-stimulated cells. These data, along with the decrease in gp130 mRNA expression in IL-6-stimulated cells, lead us to think that IL-6 signaling regulation may be mediated by other molecules, such as SOCS3, in our experimental conditions.

STAT3 is a common molecule in both IL-6 and IL-10 signaling pathways. According to our results, pSTAT3 production was enhanced by both IL-6 and IL-10 stimulation. When analyzing the effect of the combination of IL-6 + IL-10 stimulation on pSTAT3 production, a synergistic action was found: the production of pSTAT3 was more sustained in time when stimulating with the combination of cytokines, rather than with any of the cytokines alone.

Based on those results, the effect of IL-6 and IL-10 in wound healing was evaluated using an *in vitro* scratch model (Liang et al., 2007). This model allows a quantitative evaluation of the wound healing process in epithelial or endothelial cell lines by creating a cell free area, namely the scratch, and measuring the wound healing rate in response to different stimuli. Both cytokines, IL-6 and IL-10, have been described as protectors of the epithelial barrier or enhancers of the re-epithelialization (Contreras-Ruiz et al., 2012; Nakamura and Nishida, 1999).

Evaluation of the wound healing rate in different conditions revealed that the fastest wound closure happened with IL-6 stimulation, which is in accordance with previous results using rabbit cells (Nakamura and Nishida, 1999; Nishida et al., 1992a, 1992b). According to Coolen et al. (2010), a fast wound closure is in benefit of a scarless wound healing process. In the ocular surface, a fast healing process and a prompt closure of epithelial defects is important to avoid further inflammatory reactions in corneal stroma which could, in turn, lead to opacification and corneal blindness. IL-6 appears to be involved in the first phases of the re-epithelization of the cornea through the stimulation of the epithelium itself, according to Geremicca et al. (2010).

On the other hand, IL-10 exposure produced a delayed wound closure with respect to IL-6, but faster than in control cells. Considering the results of the cytokine stimulation, IL-10 probably induced an increase in gp130 and pSTAT3 expression, both of which are mediators of the IL-6 signaling pathway. Thus, the increase in these mediators would increase IL-6 signaling rate in the culture medium, achieving the same effect although delayed with regard to the direct stimulation with IL-6. Surprisingly, the role of IL-10 as protector of a scarless wound healing process has been postulated in a mouse model (Shi et al., 2013). Some species-related differences in the role of IL-10 could explain these contradictory results. Therefore, the development of three-dimensional human models of wound healing appears of great interest to elucidate the effects of different cytokines on the interaction between epithelial cells and fibroblasts or keratocytes.

In contrast, the stimulation of the scratched cultures with IL-6 + IL-10 did not produce the same synergistic effect seen in the cytokine-stimulation inflammation model, regarding pSTAT3 expression. Rather, the combination of both cytokines apparently delayed the wound healing process, since the score of wound closure was worse than after the exposure to IL-6 or to IL-10 alone. In fact, in the presence of IL-6 + IL-10, the wound closure rate was close to that of the control. STAT3 activity has been related to the wound healing process (Ekblad et al., 2013), and the wound healing rate could increase in the presence of high amounts of pSTAT3 induced by IL-6 + IL-10 stimulation. However, in the model used for this study, the opposite effect was observed. It is possible that the

evaluation of a larger scratch in the stimulation conditions of this study will lead to different results. In fact, in this work, the mean wound width was around 570 μm. In control conditions, the wound was closed after 24 h. The limitations due to the equipment available did not allow us to evaluate larger wounds. However, corneal surgical wounds are around 2 mm (Allen et al., 2012), and accidental wounds can be even bigger. Also, a higher amount of IL-10 (20 ng/ml) than of IL-6 (10 ng/ml) was used, and that might be masking the effect found when using IL-6 alone. Different concentrations of both cytokines might be used in future studies to establish a dose–response curve, in order to determine if the observed effect is maintained when modifying the amounts of the studied cytokines.

We have found no evidence of IL-6 and IL-10 acting together at the ocular surface during wound healing. To the best of our knowledge, no studies have been done so far to prove the presence of both cytokines in tears of patients with corneal injury. In this study, we have added both cytokines together, collecting no positive effects, while IL-10 has been demonstrated to protect the corneal barrier. One possible explanation may be that one of these cytokines is likely to act at the ocular surface before the other, but not at the same time. Determining the amounts of these cytokines in tears of patients at different time points after a corneal injury would help clarifying this point.

A different effect of these cytokines may also be found in *in vivo* conditions, when there is an immune system. IL-6, IL-10 or some of the mediators evaluated in this study may be considered as potential targets for therapy in corneal injury. However, the effect of IL-6 or IL-10 treatment *in vivo* should be carefully evaluated.

Published data suggest that proliferation is involved in wound healing *in vitro* (Liang et al., 2012). A study by Zhao (2007) reveals that re-epithelization can be controlled by inhibiting the PI3K signaling pathway, which is involved in proliferation. In the present study, cell proliferation was inhibited by pre-treating the cultured cells with MMC. MMC-treated cells had a slower wound closure rate than untreated cells. However, the analysis of proliferative cells percentage by EdU detection did not reveal any significant differences between the cells located at the edge of the scratch, in the different stimulation conditions. Rather, there was a greater proliferation rate in cells located in peripheral areas of the monolayer compared to that of cells in the edge of the wound. Despite this fact, the scratch was closed after 24 h in the absence of MMC. These data indicate that another mechanism besides proliferation is involved in the wound healing process *in vitro*, possibly cell migration.

Cell migration is considered by several authors as the main mechanism involved in wound healing in the scratch model (Ramaesh et al., 2012; Seet et al., 2012). In the present study, the cytoskeleton was stained to detect those migrating cells at the edges of the scratch. An α-actinin antibody was used to visualize actin fibers, and the direction of actin fibers would indicate whether the cells were migrating towards the cell-free area of the scratch or not migrating at all. Using both EdU and actin fiber staining, we saw that the cells located in the edge of the scratch were not proliferating and migrating at the same time, at least for the first hours of the study.

Although the number of proliferative cells was not increased compared to that of controls, the wound healing process was accelerated in IL-6-stimulated cells. We can say that cell migration was the main mechanism that led to wound closure in this stimulation condition. Also, after 8 h, there were greater numbers of dead cells in the cell-free area in MMC-treated cells. A possible explanation for this is that these cells may have migrated to help in the wound closure, but then died because they could not proliferate. A deeper study of migration would be necessary to better understand the events happening during wound closure.

Finally, there was an increased proliferation rate for the cells in monolayer areas distant to the wound edge after 8 h of IL-6 + IL-10-stimulated cells. This stimulatory condition led to the slowest wound closure speed, presumably increasing the risk of scarring. A higher proliferation of epithelial cells would enhance the secretion of extracellular matrix into the wound, leading to scarring. To test this hypothesis the development of a three-dimensional model of wound healing, with fibroblasts and epithelial cells co-culture, would be warranted.

In this study we have demonstrated that both IL-6 and IL-10 are involved in the wound healing response, but not synergistically. IL-6 stimulation leaded to the fastest wound healing rate, although the presence of IL-10 inhibited the potential positive effect of IL-6, in the *in vitro* corneal scratch assay. In it, wound closure is the result of the combination of cell proliferation and cell migration.

Acknowledgments

Authors would like to thank Mª Cruz Valsero Blanco, PhD, for statistical analysis support. Authors also acknowledge the assistance of Britt Bromberg, PhD, ELS, of Xenofile Editing (http://www.xenofileediting.com) for the editing of the manuscript. This work was supported by Grant code FEDER-CICYT MAT2010-20452-C03-01. Isabel Arranz-Valsero was supported by Regional JCyL Scholarship/European Social Fund Program and other authors by FPI Scholarship Programs (Ministry of Science and Innovation, and University of Valladolid, Spain). None of the authors have commercial interest in the results of this manuscript. This work has been included in an academic thesis work and partially presented at the Association for Ocular Pharmacology and Therapeutics (AOPT) 2013 Scientific Meeting (Alicante, Spain).

References

Allen, D., Habib, M., Steel, D., 2012. Final incision size after implantation of a hydrophobic acrylic aspheric intraocular lens: new motorized injector versus standard manual injector. J. Cataract Refract. Surg. 38, 249–255.

Araki-Sasaki, K., Ohashi, Y., Sasabe, T., Hayashi, K., Watanabe, H., Tano, Y., Handa, H., 1995. An SV40-immortalized human corneal epithelial cell line and its characterization. Investig. Ophthalmol. Vis. Sci. 36, 614–621.

Aurora, A.L., 1979. Corneal blindness—a review. Indian J. Ophthalmol. 27, 1–14.

Baudouin, C., Hamard, P., Liang, H., Creuzot-Garcher, C., Bensoussan, L., Brignole, F., 2004. Conjunctival epithelial cell expression of interleukins and inflammatory markers in glaucoma patients treated over the long term. Ophthalmology 111, 2186–2192.

Benowitz, L.I., Popovich, P.G., 2011. Inflammation and axon regeneration. Curr. Opin. Neurol. 24, 577–583.

Bonetto, A., Aydogdu, T., Jin, X., Zhang, Z., Zhan, R., Puzis, L., Koniaris, L.G., Zimmers, T.A., 2012. JAK/STAT3 pathway inhibition blocks skeletal muscle wasting downstream of IL-6 and in experimental cancer cachexia. Am. J. Physiol. Endocrinol. Metab. 303, E410–E421.

Boorstein, S.M., Elner, S.G., Meyer, R.F., Sugar, A., Strieter, R.M., Kunkel, S.L., Elner, V.M., 1994. Interleukin-10 inhibition of HLA-DR expression in human herpes stromal keratitis. Ophthalmology 101, 1529–1535.

Cassoux, N., Giron, A., Bodaghi, B., Tran, T.H., Baudet, S., Davy, F., Chan, C.C., Lehoang, P., Merle-Beral, H., 2007. IL-10 measurement in aqueous humor for screening patients with suspicion of primary intraocular lymphoma. Investig. Ophthalmol. Vis. Sci. 48, 3253–3259.

Contreras-Ruiz, L., Schulze, U., Garcia-Posadas, L., Arranz-Valsero, I., Lopez-Garcia, A., Paulsen, F., Diebold, Y., 2012. Structural and functional alteration of corneal epithelial barrier under inflammatory conditions. Curr. Eye Res. 37, 971–981.

Coolen, N.A., Schouten, K.C., Boekema, B.K., Middelkoop, E., Ulrich, M.M., 2010. Wound healing in a fetal, adult, and scar tissue model: a comparative study. Wound Repair Regen. 18, 291–301.

Darnell Jr., J.E., 1997. STATs and gene regulation. Science 277, 1630–1635.

de Waal Malefyt, R., Abrams, J., Bennett, B., Figdor, C.G., de Vries, J.E., 1991. Interleukin 10(IL-10) inhibits cytokine synthesis by human monocytes: an autoregulatory role of IL-10 produced by monocytes. J. Exp. Med. 174, 1209–1220.

Eckes, B., Zigrino, P., Kessler, D., Holtkotter, O., Shephard, P., Mauch, C., Krieg, T., 2000. Fibroblast-matrix interactions in wound healing and fibrosis. Matrix Biol. 19, 325–332.

Ekblad, L., Lindgren, G., Persson, E., Kjellen, E., Wennerberg, J., 2013. Cell-line-specific stimulation of tumor cell aggressiveness by wound healing factors - a central role for STAT3. BMC Cancer 13, 33–2407-13-33.
Enriquez-de-Salamanca, A., Calder, V., Gao, J., Galatowicz, G., Garcia-Vazquez, C., Fernandez, I., Stern, M.E., Diebold, Y., Calonge, M., 2008. Cytokine responses by conjunctival epithelial cells: an in vitro model of ocular inflammation. Cytokine 44, 160–167.
Enriquez-de-Salamanca, A., Castellanos, E., Stern, M.E., Fernandez, I., Carreno, E., Garcia-Vazquez, C., Herreras, J.M., Calonge, M., 2010. Tear cytokine and chemokine analysis and clinical correlations in evaporative-type dry eye disease. Mol. Vis. 16, 862–873.
Ferrari, G., Bignami, F., Giacomini, C., Franchini, S., Rama, P., 2013. Safety and efficacy of topical infliximab in a mouse model of ocular surface scarring. Investig. Ophthalmol. Vis. Sci. 54, 1680–1688.
Filbin, M.T., 2006. How inflammation promotes regeneration. Nat. Neurosci. 9, 715–717.
Geremicca, W., Fonte, C., Vecchio, S., 2010. Blood components for topical use in tissue regeneration: evaluation of corneal lesions treated with platelet lysate and considerations on repair mechanisms. Blood Transfus. 8, 107–112.
Ghasemi, H., Ghazanfari, T., Yaraee, R., Owlia, P., Hassan, Z.M., Faghihzadeh, S., 2012. Roles of IL-10 in ocular inflammations: a review. Ocul. Immunol. Inflamm. 20, 406–418.
Heinrich, P.C., Behrmann, I., Muller-Newen, G., Schaper, F., Graeve, L., 1998. Interleukin-6-type cytokine signalling through the gp130/Jak/STAT pathway. Biochem. J. 334 (Pt 2), 297–314.
Leonardi, A., Motterle, L., Bortolotti, M., 2008. Allergy and the eye. Clin. Exp. Immunol. 153 (Suppl 1), 17–21.
Lewis, A.C., 2013. Interleukin-6 in the pathogenesis of posterior capsule opacification and the potential role for interleukin-6 inhibition in the future of cataract surgery. Med. Hypotheses 80, 466–474.
Liang, C.C., Park, A.Y., Guan, J.L., 2007. In vitro scratch assay: a convenient and inexpensive method for analysis of cell migration in vitro. Nat. Protoc. 2, 329–333.
Liang, H., Baudouin, C., Daull, P., Garrigue, J.S., Buggage, R., Brignole-Baudouin, F., 2012. In vitro and in vivo evaluation of a preservative-free cationic emulsion of latanoprost in corneal wound healing models. Cornea 31, 1319–1329.
Lockwood, A., Brocchini, S., Khaw, P.T., 2013. New developments in the pharmacological modulation of wound healing after glaucoma filtration surgery. Curr. Opin. Pharmacol. 13, 65–71.
Lu, X., Richardson, P.M., 1991. Inflammation near the nerve cell body enhances axonal regeneration. J. Neurosci. 11, 972–978.
Micera, A., Lambiase, A., Puxeddu, I., Aloe, L., Stampachiacchiere, B., Levi-Schaffer, F., Bonini, S., Bonini, S., 2006. Nerve growth factor effect on human primary fibroblastic-keratocytes: possible mechanism during corneal healing. Exp. Eye Res. 83, 747–757.
Mochizuki, M., Sugita, S., Kamoi, K., 2013. Immunological homeostasis of the eye. Prog. Retin. Eye Res. 33, 10–27.
Nakamura, M., Nishida, T., 1999. Differential effects of epidermal growth factor and interleukin 6 on corneal epithelial cells and vascular endothelial cells. Cornea 18, 452–458.
Nathan, C., 2002. Points of control in inflammation. Nature 420, 846–852.
Nishida, T., Nakamura, M., Mishima, H., Otori, T., 1992a. Interleukin 6 promotes epithelial migration by a fibronectin-dependent mechanism. J. Cell. Physiol. 153, 1–5.
Nishida, T., Nakamura, M., Mishima, H., Otori, T., Hikida, M., 1992b. Interleukin 6 facilitates corneal epithelial wound closure in vivo. Arch. Ophthalmol. 110, 1292–1294.
Oh, J.Y., Roddy, G.W., Choi, H., Lee, R.H., Ylostalo, J.H., Rosa Jr., R.H., Prockop, D.J., 2010. Anti-inflammatory protein TSG-6 reduces inflammatory damage to the cornea following chemical and mechanical injury. Proc. Natl. Acad. Sci. U. S. A. 107, 16875–16880.
Ramaesh, T., Ramaesh, K., Riley, S.C., West, J.D., Dhillon, B., 2012. Effects of N-acetylcysteine on matrix metalloproteinase-9 secretion and cell migration of human corneal epithelial cells. Eye (Lond) 26, 1138–1144.
Romagnani, P., Crescioli, C., 2012. CXCL10: a candidate biomarker in transplantation. Clin. Chim. Acta 413, 1364–1373.
Seet, L.F., Su, R., Toh, L.Z., Wong, T.T., 2012. In vitro analyses of the anti-fibrotic effect of SPARC silencing in human Tenon's fibroblasts: comparisons with mitomycin C. J. Cell. Mol. Med. 16, 1245–1259.
Seibold, L.K., Sherwood, M.B., Kahook, M.Y., 2012. Wound modulation after filtration surgery. Surv. Ophthalmol. 57, 530–550.
Shi, J.H., Guan, H., Shi, S., Cai, W.X., Bai, X.Z., Hu, X.L., Fang, X.B., Liu, J.Q., Tao, K., Zhu, X.X., Tang, C.W., Hu, D.H., 2013. Protection against TGF-beta1-induced fibrosis effects of IL-10 on dermal fibroblasts and its potential therapeutics for the reduction of skin scarring. Arch. Dermatol. Res. 305, 341–352.
Silver, J.S., Hunter, C.A., 2010. Gp130 at the nexus of inflammation, autoimmunity, and cancer. J. Leukoc. Biol. 88, 1145–1156.
Subramaniam, A., Shanmugam, M.K., Perumal, E., Li, F., Nachiyappan, A., Dai, X., Swamy, S.N., Ahn, K.S., Kumar, A.P., Tan, B.K., Hui, K.M., Sethi, G., 2013. Potential role of signal transducer and activator of transcription (STAT)3 signaling pathway in inflammation, survival, proliferation and invasion of hepatocellular carcinoma. Biochim. Biophys. Acta 1835, 46–60.
Traum, D., Timothee, P., Silver, J., Rose-John, S., Ernst, M., LaRosa, D.F., 2012. IL-10-induced gp130 expression in mouse mast cells permits IL-6 trans-signaling. J. Leukoc. Biol. 91, 427–435.
Ueta, M., Kinoshita, S., 2012. Ocular surface inflammation is regulated by innate immunity. Prog. Retin. Eye Res. 31, 551–575.
van Gelderen, B.E., Van Der Lelij, A., Peek, R., Broersma, L., Treffers, W.F., Ruijter, J.M., van Der Gaag, R., 2000. Cytokines in aqueous humour and serum before and after corneal transplantation and during rejection. Ophthalmic Res. 32, 157–164.
Ward, L.D., Hammacher, A., Howlett, G.J., Matthews, J.M., Fabri, L., Moritz, R.L., Nice, E.C., Weinstock, J., Simpson, R.J., 1996. Influence of interleukin-6 (IL-6) dimerization on formation of the high affinity hexameric IL-6.receptor complex. J. Biol. Chem. 271, 20138–20144.
Yang, Y., Yang, H., Wang, Z., Mergler, S., Wolosin, J.M., Reinach, P.S., 2013. Functional TRPV1 expression in human corneal fibroblasts. Exp. Eye Res. 107, 121–129.
Zhao, M., 2007. PTEN: a promising pharmacological target to enhance epithelial wound healing. Br. J. Pharmacol. 152, 1141–1144.